

# A theoretical study on the ionization of tetrafluoroethylene with analysis of vibrational structure of the photoelectron spectra

**Kouichi Takeshita**

Faculty of Bioindustry, Tokyo University of Agriculture, Abashiri, Hokkaido 099-24, Japan

Received June 12, 1995/Final revision received November 14, 1995/Accepted November 14, 1995

**Abstract.** *Ab initio* calculations have been performed to study on the molecular structures and the vibrational levels of the low-lying ionic states ( ${}^2B_{2u}$ ,  ${}^2A_g$ ,  ${}^2B_{2g}$ ,  ${}^2B_{3u}$ ,  ${}^2A_u$ ,  ${}^2B_{1g}$ ,  ${}^2B_{1u}$ , and  ${}^2B_{3g}$ ) of tetrafluoroethylene. The equilibrium molecular structures and vibrational modes of these states are presented. The theoretical ionization intensity curves including the vibrational structures of the low-lying eight ionic states are also presented and compared with the photoelectron spectrum. Some new assignments of the photoelectron spectra are proposed.

**Key words:**  $C_2F_4^+$  – RHF/gradient – Molecular structure – Vibrational analysis – Franck–Condon factor – PE-spectrum

## 1. Introduction

The electronic configuration of the ground state of tetrafluoroethylene is represented by a  $\dots (1b_{3g})^2 (5b_{1u})^2 (1b_{1g})^2 (1a_u)^2 (4b_{3u})^2 (4b_{2g})^2 (6a_g)^2 (2b_{2u})^2$  with the  $D_{2h}$  symmetry group by the coordinate axis illustrated in Fig. 1. The  $1b_{3g}$ ,  $5b_{1u}$ ,  $1b_{1g}$ ,  $1a_u$ ,  $4b_{3u}$ ,  $4b_{2g}$ ,  $6a_g$ , and  $2b_{2u}$  MOs are illustrated in Figs. 2 and 3. The  $2b_{2u}$  is a  $\pi$  MO. The  $6a_g$ ,  $4b_{2g}$ ,  $4b_{3u}$ , and  $5b_{1u}$  MOs are nonbonding orbitals formed by the  $2P_x$  and  $2p_z$  AOs of F's. The  $1a_u$ ,  $1b_{1g}$  and  $1b_{3g}$  MOs are nonbonding orbitals formed by the  $2P_y$  AO's of F's.

The photoelectron (PE) spectroscopy investigations of tetrafluoroethylene have been reported by many workers [1–5]. Five separated bands have been observed below 19.0 eV. The first band has been observed in the 10.10–11.8 eV region. It has been assigned to the  ${}^2B_{2u}$  state. It has showed a well resolved vibrational structure. An interpretation of the vibrational structure has been reported by Brundle et al. [2]. The four separated bands have been found in the 16–18 eV region. In order to assign the electronic states of these bands, Brundle et al. have calculated the ionization energies by using corrected Koopmans' theorem and found six electronic states in this region. However, they could not establish the assignment, because several states have been predicated to be close together. The band found at 17.6 eV has showed the vibrational structure. An interpretation of the vibrational structure has been reported by Brundle et al.

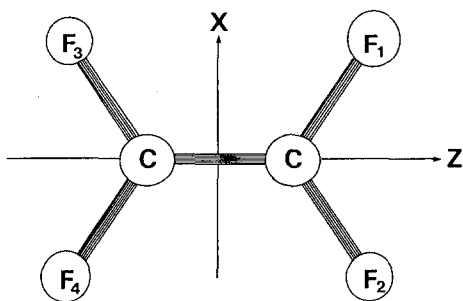


Fig. 1. A definition of the coordinate axis

The theoretical approaches on tetrafluoroethylene have been reported [2, 4, 6]. Many workers have calculated the vertical ionization energies to help the assignment of the electronic states of the PE spectra. The vertical ionization energy has been calculated by using the molecular structure of the ground state.

A position of a band depends on the ionization energy and a shape of a band depends on the vibrational structure. As a molecule is ionized, the equilibrium molecular structure and the character of the vibrational mode should change from those of the ground state. The ionization energy and vibrational structure of the PE spectrum reflect these changes. It is significant to investigate the ionization energy and vibrational structure associated with the change in the equilibrium molecular structure and the vibrational mode by ionization.

No theoretical investigation on the molecular structures and the vibrational levels of the ionic states has been reported. In this work, we determine the equilibrium molecular structures of the ground and lower eight ionic states ( ${}^2B_{2u}$ ,  ${}^2A_g$ ,  ${}^2B_{2g}$ ,  ${}^2B_{3u}$ ,  ${}^2A_u$ ,  ${}^2B_{1g}$ ,  ${}^2B_{1u}$ , and  ${}^2B_{3g}$ ) by using the *ab initio* self-consistent-field (SCF) method. Within the framework of the adiabatic approximation and the harmonic oscillator approximation, we have calculated the harmonic force constant matrix elements over variables of the totally symmetric distortion and the vibrational frequencies of the totally symmetric distortion and the vibrational frequencies of the totally symmetric modes. We have obtained approximate theoretical intensity curves using the Franck-Condon factor (FCF), which is given by the square of the overlap integrals between the vibrational wave function of the ground state and that of the ionic state. Based on these calculations, we discuss the assignment of the electronic state of the band and that of the vibrational structure compared to the photoelectron spectrum.

## 2. Method of calculations

We have used the split valence type basis sets of the MIDI-4-type prepared by Tatewaki and Huzinaga [7]. These are augmented by one *p*-type polarization function for H and one *d*-type polarization function for C and F. The exponents of the polarization function for H, C, and F are 0.68, 0.61, and 1.50, respectively.

The gradient technique for the Roothaan's restricted Hartree-Fock (RHF) method has been applied to find the optimum molecular structures of the ground and ionic states.

The single and double excitation configuration interaction (SDCI) method has been used to get more accurate ionization energies for the estimation of vertical ionization (VI) energy and adiabatic ionization (AI) energy. We have used a single

reference configuration of the RHF wave function of the respective state. In the SDCl method, singly and doubly excited configuration state functions (CSFs) have been generated where the inner shells have been kept frozen. The number of the generated CSFs of the ground state is 75 553 and those of the ionic states are about 175 000.

The harmonic force constant matrix elements have been calculated by the gradient technique with the RHF wave function; the second derivative has been estimated by the numerical differentiation of the analytically calculated first derivative. We have calculated the FCFs of only the totally symmetric vibrational modes. In calculating FCFs, we have approximated the vibrational wave functions by those obtained by the harmonic oscillator model. We have assumed that the initial state has been the zero point vibrational level of the ground state. The method of calculation of the FCF and theoretical intensity curves is the same as we used in the previous paper [8].

This work has been carried out by using the computer program system GRAMOL [9] for the gradient technique and the calculation of normal modes, and ALCHEMY II [10–12] for the CI calculations.

### 3. Results and discussion

Table 1 shows the optimized geometrical parameters of the ground and ionic states. The optimized geometric parameters of the ground state are in good agreement with the experimental ones [13]. Table 1 also shows a magnitude of the change in the equilibrium molecular structure by ionization.

Table 2 shows the VI and AI energies at the SCF and SDCl levels. In the SDCl calculations, the weights of the reference function are 84–86% at the optimized geometry. Each contribution of another CSF is less than 1.0%. Bieri et al. [5] have reported the VIEs by means of many-body Green's function calculations. The results are given in the footnote of Table 1. The ordering of the VIEs by Bieri et al. is consistent with the present calculations.

**Table 1.** Optimized molecular structure and magnitude of the change in the geometry by ionization

| State             | C=C ( $\Delta C=C$ ) | C-F ( $\Delta C-F$ ) | C=C-F ( $\Delta C=C-F$ ) |
|-------------------|----------------------|----------------------|--------------------------|
| $^1A_g$           | 1.303                | 1.297                | 123.54                   |
| Obs. <sup>a</sup> | 1.311                | 1.319                | 123.76                   |
| $^2B_{2u}$        | 1.400 (+ 0.097)      | 1.241 (– 0.056)      | 120.84 (– 2.70)          |
| $^2A_g$           | 1.386 (+ 0.083)      | 1.265 (– 0.032)      | 118.06 (– 5.48)          |
| $^2B_{2g}$        | 1.288 (– 0.015)      | 1.294 (– 0.003)      | 125.73 (+ 2.19)          |
| $^2B_{3u}$        | 1.295 (– 0.008)      | 1.302 (+ 0.005)      | 127.36 (+ 3.82)          |
| $^2A_u$           | 1.295 (– 0.008)      | 1.302 (+ 0.005)      | 124.47 (+ 0.93)          |
| $^2B_{1g}$        | 1.299 (– 0.004)      | 1.304 (+ 0.007)      | 125.05 (+ 1.51)          |
| $^2B_{1u}$        | 1.279 (– 0.024)      | 1.316 (+ 0.019)      | 121.01 (– 2.53)          |
| $^2B_{3g}$        | 1.288 (– 0.015)      | 1.325 (+ 0.028)      | 122.67 (– 0.87)          |

<sup>a</sup> Ref. [13]

Bond lengths are in angstroms, angles in degrees

The values in parenthesis are the magnitudes of the change in geometry by ionization

**Table 2.** Ionization energies (eV)

| State               | VIE   |       | AIE   |       | $\Delta(\text{VIE}-\text{AIE})$ |      | O–O transition |       |
|---------------------|-------|-------|-------|-------|---------------------------------|------|----------------|-------|
|                     | SCF   | SDCI  | SCF   | SDCI  | SCF                             | SDCI | O–O IE         | FCF   |
| ${}^2\text{B}_{2u}$ | 9.74  | 10.32 | 8.99  | 9.67  | 0.75                            | 0.65 | 9.67           | 0.031 |
| ${}^2\text{A}_g$    | 17.53 | 17.08 | 17.09 | 16.82 | 0.44                            | 0.26 | 16.79          | 0.006 |
| ${}^2\text{B}_{2g}$ | 17.61 | 16.93 | 17.55 | 16.91 | 0.06                            | 0.02 | 16.92          | 0.362 |
| ${}^2\text{B}_{3u}$ | 18.07 | 17.44 | 17.88 | 17.25 | 0.19                            | 0.19 | 17.26          | 0.031 |
| ${}^2\text{A}_u$    | 18.57 | 17.77 | 18.56 | 17.76 | 0.01                            | 0.01 | 17.76          | 0.841 |
| ${}^2\text{B}_{1g}$ | 18.77 | 17.95 | 18.73 | 17.91 | 0.04                            | 0.04 | 17.91          | 0.580 |
| ${}^2\text{B}_{1u}$ | 19.46 | 18.69 | 19.31 | 18.51 | 0.15                            | 0.18 | 18.52          | 0.092 |
| ${}^2\text{B}_{3g}$ | 20.26 | 19.44 | 20.14 | 19.25 | 0.12                            | 0.19 | 19.25          | 0.378 |

Total energies (a.u.) of  ${}^1\text{A}_g$ :  $-472.930060$  (SCF) and  $-473.776258$  (SDCI)

VIE: Vertical ionization energy

AIE: Adiabatic ionization energy defined as the energy from the bottom to the bottom of the potential curves

O–O IE: O–O ionization energy defined as the energy from the zero point vibrational level of the ground state to that of the ionic state

Bieri et al. [5] have reported the VIE by means of many-body Green's function calculations as follows: VIEs of the  ${}^2\text{B}_{2u}$ ,  ${}^2\text{B}_{2g}$ ,  ${}^2\text{A}_g$ ,  ${}^2\text{B}_{3u}$ ,  ${}^2\text{A}_u$ ,  ${}^2\text{B}_{1g}$ ,  ${}^2\text{B}_{1u}$ , and  ${}^2\text{B}_{3g}$  states are 11.10, 16.62, 16.75, 17.04, 17.27, 17.42, 18.12, and 18.87 eV, respectively

Table 2 shows the energy lowering of the AI energy compared with the VI energy. A large energy lowering is found in the  ${}^2\text{B}_{2u}$  state corresponding to the large change in the equilibrium molecular structure. While the energy lowering of the  ${}^2\text{B}_{2g}$ ,  ${}^2\text{A}_u$ , and  ${}^2\text{B}_{1g}$  states are negligibly small. The O–O ionization energies and the FCFs of the O–O transitions are listed in Table 2. The FCF of the  ${}^2\text{B}_{2u}$  state is so large that the O–O transition should be observed. Brundle et al. have reported that the observed O–O band of the  ${}^2\text{B}_{2u}$  state has been 10.10 eV. The present calculated value is underestimated by 0.43 eV in comparison with their value.

The vibrational frequencies of the ground and ionic states are shown in Table 3. The frequencies are arranged in order of magnitude. Comparing with the observed values [14] of the  ${}^1\text{A}_1$  state, we overestimate the frequencies by 9.9–14.6%. Each mode is characterized by using the conventional potential energy distribution (PED) [15] and the classical half-amplitude of the zero-point vibrational levels. Table 3 includes the PED of the C=C stretching mode, C–F stretching mode and C=C–F bending mode. The classical half-amplitude is shown in Table 4.

Table 3 shows that the  $\nu_1$  and  $\nu_2$  modes of the  ${}^1\text{A}_g$  state are characterized mainly as the C=C and C–F stretching motions, respectively. It also shows that the C–F and C=C stretching motions contribute to the  $\nu_1$  and  $\nu_2$  modes, respectively. Table 4 suggests that the characters of the  $\nu_1$  and  $\nu_2$  modes are the mixtures of the C=C and C–F stretching motions. The C=C and C–F stretching motions couple with the out-of-phase in the  $\nu_1$  mode and with the in-phase in the  $\nu_2$  mode. The  $\nu_3$  mode is interpreted as the C=C–F bending motion.

For the ionic states, the characters of the  $\nu_1$ ,  $\nu_2$  and  $\nu_3$  modes of all states correspond generally to those of the ground state. A small change of the PED and the classical half-amplitude is found in the  $\nu_1$  and  $\nu_2$  modes of the  ${}^2\text{B}_{2u}$  and  ${}^2\text{A}_g$  states. It is also found from Table 3 that some obvious changes in frequencies

**Table 3.** Vibrational frequencies ( $\text{cm}^{-1}$ ) and Potential Energy Distributions

| State      | Mode    | Vibrational frequency | Potential energy distribution (%) |
|------------|---------|-----------------------|-----------------------------------|
| $^1A_g$    | $\nu_1$ | 2145                  | C=C (68), C-F (24), C=C-F (9)     |
|            | $\nu_2$ | 874                   | C-F (78), C=C (18), C=C-F (5)     |
|            | $\nu_3$ | 433                   | C=C-F (90), C=C (9), C-F (1)      |
| $^2B_{2u}$ | $\nu_1$ | 1958                  | C=C (51), C-F (37), C=C-F (12)    |
|            | $\nu_2$ | 914                   | C-F (60), C=C (28), C=C-F (11)    |
|            | $\nu_3$ | 443                   | C=C-F (82), C=C (17), C-F (1)     |
| $^2A_g$    | $\nu_1$ | 1528                  | C=C (55), C-F (33), C=C-F (11)    |
|            | $\nu_2$ | 878                   | C-F (58), C=C (32), C=C-F (9)     |
|            | $\nu_3$ | 411                   | C=C-F (96), C=C (3), C-F (2)      |
| $^2B_{2g}$ | $\nu_1$ | 2243                  | C=C (69), C-F (25), C=C-F (6)     |
|            | $\nu_2$ | 858                   | C-F (76), C=C (21), C=C-F (3)     |
|            | $\nu_3$ | 374                   | C=C-F (92), C=C (7), C-F (1)      |
| $^2B_{3u}$ | $\nu_1$ | 2218                  | C=C (67), C-F (26), C=C-F (7)     |
|            | $\nu_2$ | 849                   | C-F (74), C=C (21), C=C-F (5)     |
|            | $\nu_3$ | 426                   | C=C-F (91), C=C (8), C-F (2)      |
| $^2A_u$    | $\nu_1$ | 2196                  | C=C (68), C-F (24), C=C-F (7)     |
|            | $\nu_2$ | 858                   | C-F (77), C=C (19), C=C-F (4)     |
|            | $\nu_3$ | 404                   | C=C-F (91), C=C (8), C-F (1)      |
| $^2B_{1g}$ | $\nu_1$ | 2177                  | C=C (68), C-F (24), C=C-F (8)     |
|            | $\nu_2$ | 855                   | C-F (77), C=C (19), C=C-F (4)     |
|            | $\nu_3$ | 418                   | C=C-F(91), C=C(8), C-F(1)         |
| $^2B_{1u}$ | $\nu_1$ | 2238                  | C=C (74), C-F (19), C=C-F (7)     |
|            | $\nu_2$ | 853                   | C-F (82), C=C (15), C=C-F (3)     |
|            | $\nu_3$ | 380                   | C=C-F (92), C=C (8), C-F (1)      |
| $^2B_{3g}$ | $\nu_1$ | 2194                  | C=C (72), C-F (20), C=C-F (7)     |
|            | $\nu_2$ | 840                   | C-F (81), C=C (16), C=C-F (3)     |
|            | $\nu_3$ | 395                   | C=C-F (92), C=C (7), C-F (1)      |

Observed vibrational frequencies [14] of  $\nu_1$ ,  $\nu_2$ , and  $\nu_3$  are 1872, 778, and  $394 \text{ cm}^{-1}$ , respectively

are found in the  $\nu_1$  mode of these states. The frequencies decrease. This should be connected with the fact that the C=C distance lengthens and the C=F distance shortens by ionization.

It is found from Table 4 that the magnitudes of the classical half-amplitude of the C=C stretching, C-F stretching and C=C-F bending motions are about 0.05 Å, 0.018 Å, and  $1.3^\circ$ , respectively. Comparing these magnitudes with the changes in the equilibrium molecular structure by ionization, we find some significant changes in the C=C distance of the  $^2B_{2u}$  and  $^2A_g$  states, C-F distance of the  $^2B_{2u}$ ,  $^2A_g$ , and  $^2B_{3g}$  states, and C=C-F angle of the  $^2B_{2u}$ ,  $^2A_g$ ,  $^2B_{2g}$ ,  $^2B_{3u}$ , and  $^2B_{1u}$  states. For the  $^2A_u$  and  $^2B_{1g}$  states, each change in the equilibrium geometrical parameter is negligibly small compared to the magnitude of the classical half-amplitude. This situation should be connected with a small energy lowering of the AI energy compared with the VI energy and with a large value of the FCF of the O-O transition. The overall feature of the theoretical intensity curves of the  $^2B_{2u}$ ,

**Table 4.** Classical half amplitude of the zero-point vibrational levels

| State      | Component      | $\nu_1$ | $\nu_2$ | $\nu_3$ |
|------------|----------------|---------|---------|---------|
| $^1A_g$    | $\Delta C=C$   | 0.050   | 0.015   | 0.008   |
|            | $\Delta C-F$   | -0.017  | 0.018   | 0.001   |
|            | $\Delta C=C-F$ | -1.0    | -0.4    | 1.3     |
| $^2B_{2u}$ | $\Delta C=C$   | 0.051   | 0.024   | 0.013   |
|            | $\Delta C-F$   | -0.018  | 0.015   | 0.001   |
|            | $\Delta C=C-F$ | -1.0    | -0.6    | 1.2     |
| $^2A_g$    | $\Delta C=C$   | 0.057   | 0.026   | 0.005   |
|            | $\Delta C-F$   | -0.019  | 0.015   | 0.002   |
|            | $\Delta C=C-F$ | -1.2    | -0.6    | 1.4     |
| $^2B_{2g}$ | $\Delta C=C$   | 0.049   | 0.016   | 0.006   |
|            | $\Delta C-F$   | -0.017  | 0.018   | 0.002   |
|            | $\Delta C=C-F$ | -0.9    | -0.4    | 1.4     |
| $^2B_{3u}$ | $\Delta C=C$   | 0.049   | 0.016   | 0.007   |
|            | $\Delta C-F$   | -0.018  | 0.017   | 0.002   |
|            | $\Delta C=C-F$ | -0.9    | -0.4    | 1.3     |
| $^2A_u$    | $\Delta C=C$   | 0.050   | 0.015   | 0.007   |
|            | $\Delta C-F$   | -0.017  | 0.018   | 0.001   |
|            | $\Delta C=C-F$ | -0.9    | -0.4    | 1.3     |
| $^2B_{1g}$ | $\Delta C=C$   | 0.050   | 0.015   | 0.007   |
|            | $\Delta C-F$   | -0.017  | 0.018   | 0.002   |
|            | $\Delta C=C-F$ | -0.9    | -0.4    | 1.3     |
| $^2B_{1u}$ | $\Delta C=C$   | 0.049   | 0.013   | 0.006   |
|            | $\Delta C-F$   | -0.015  | 0.019   | 0.001   |
|            | $\Delta C=C-F$ | -0.9    | -0.3    | 1.4     |
| $^2B_{3g}$ | $\Delta C=C$   | 0.050   | 0.014   | 0.007   |
|            | $\Delta C-F$   | -0.016  | 0.019   | 0.001   |
|            | $\Delta C=C-F$ | -0.9    | -0.4    | 1.3     |

Bond lengths are in angstroms, angles in degrees

$^2A_g$ ,  $^2B_{2g}$ ,  $^2B_{3u}$ ,  $^2A_u$ ,  $^2B_{1g}$ ,  $^2B_{1u}$ , and  $^2B_{3g}$  states are illustrated in Fig. 4 by assuming a half-width of 0.08 eV for each transition band. It is compared with the observed PE spectrum by Bieri et al. [5]. It reproduces well the observed PE spectrum. In order to discuss more detailed vibrational structure of each band and the contribution of each band to the spectrum, we illustrate the theoretical intensity curve with a half-width of 0.02 eV. The results are shown in Figs. 5–12. The interpretations of the vibrational structures are given in the Figs. 9 and 10, and Tables 5–10.

Figure 5 illustrates the theoretical intensity curve of the  $^2B_{2u}$  state and the observed PE spectrum of Brundle et al. [2]. A well resolved vibrational structure is found in both spectra. The vibrational structure of the theoretical intensity curve reproduces well that of the PE spectrum. Three vibrational progressions of A, B, and C are found. An assignment of each progression is found in Table 5. The progression A with strong intensity is a series of the vibrational excitations of (000)–(600). The progression B with weak intensity is a series of (001)–(501) and the progression on C with medium intensity is a series of (010)–(610).

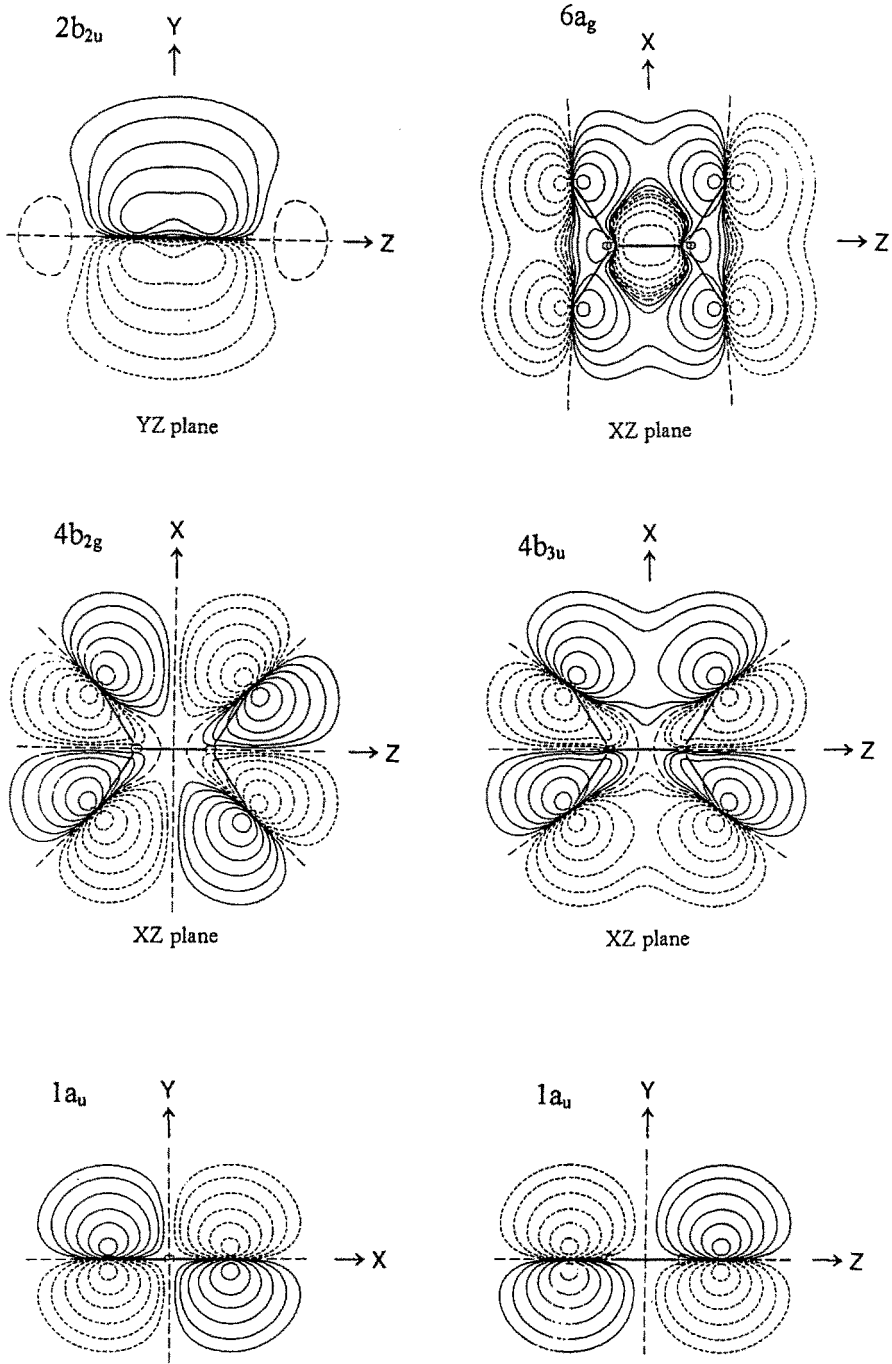


Fig. 2. The 2b<sub>2u</sub>, 6a<sub>g</sub>, 4b<sub>2g</sub>, 4b<sub>3u</sub>, and 1a<sub>u</sub> MOs

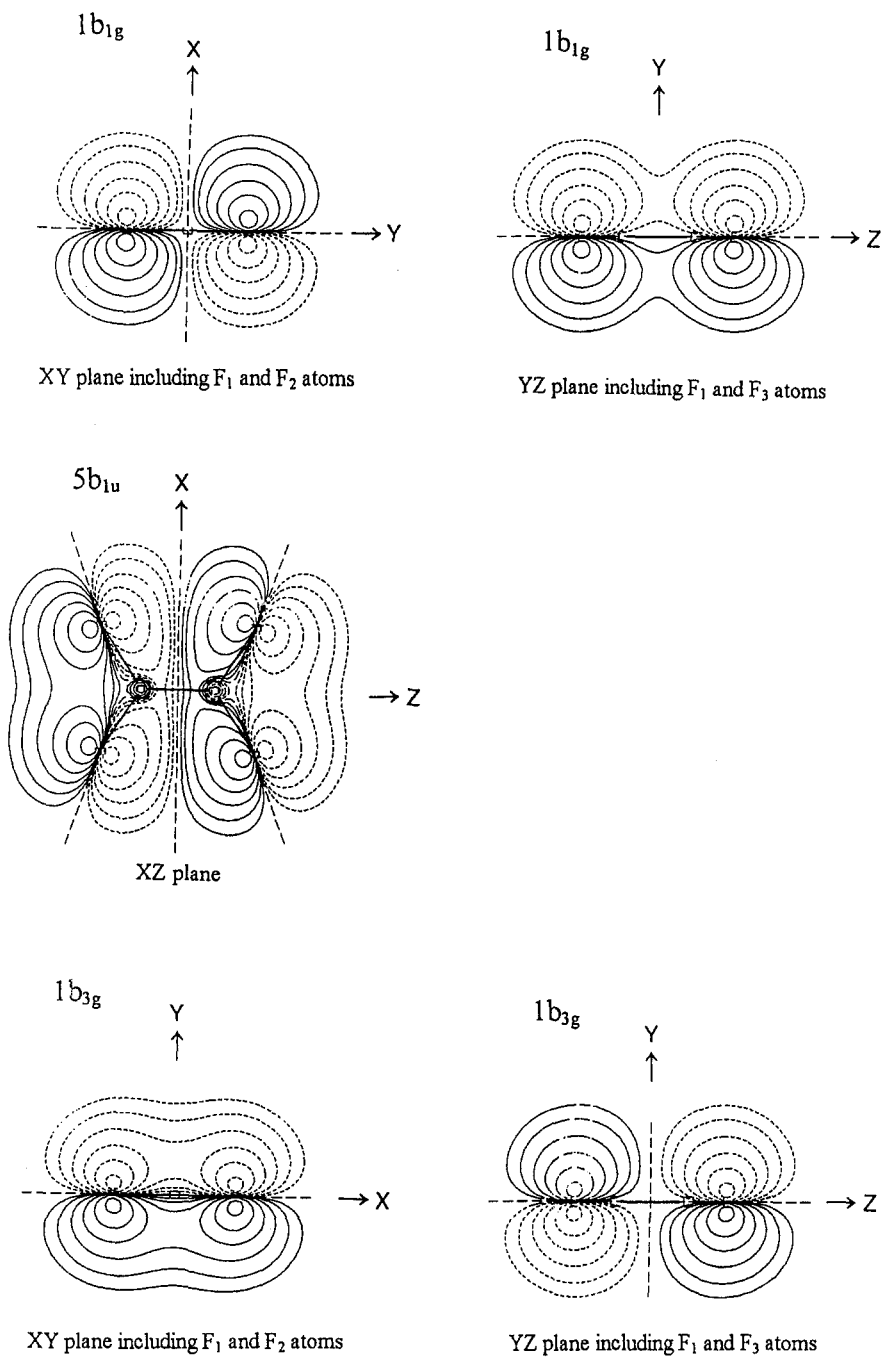
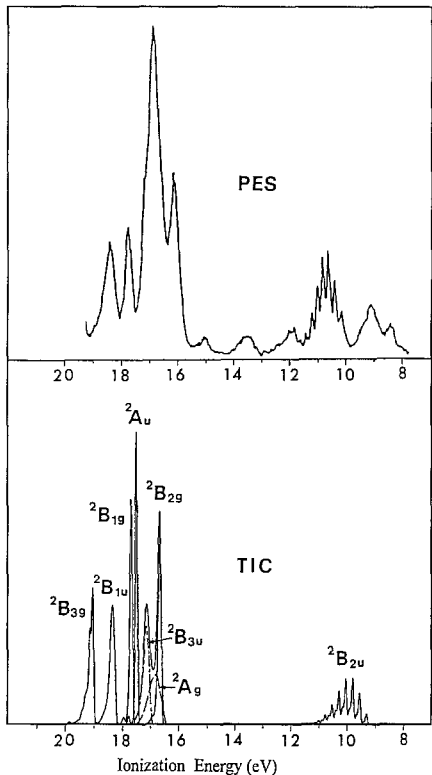


Fig. 3. The  $1b_{1g}$ ,  $5b_{1u}$  and  $1b_{3g}$  MOs





**Fig. 4**

**Fig. 4.** The total feature of the theoretical intensity curves of ionization with a half-width of 0.08 eV and the observed photoelectron spectrum by Bieri et al. [5]. TIC: Theoretical intensity curve and PES: PE spectrum

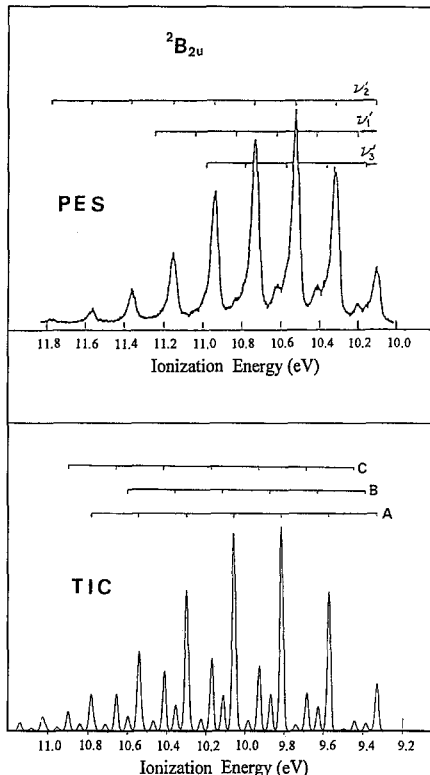


**Fig. 5**

**Fig. 5.** The theoretical intensity curves of ionization of the  $^2B_{2u}$  state with a half-width of 0.02 eV and the observed photoelectron spectrum by Brundle et al. [2]. They used the following notation of the vibrational mode:  $\nu_1$  (C-F stretch),  $\nu_2$  (C=C stretch), and  $\nu_3$  ( $F_2C$  scissors). TIC: Theoretical intensity curve and PES: PE spectrum

Brundle et al. have interpreted the vibrational structure of the PE spectrum. Their interpretation of the vibrational progressions of the lower energy side is the same as the present result except for a notation of each vibrational mode. They have used the notation as follows:  $\nu_1$  (C-F stretch),  $\nu_2$  (C=C stretch), and  $\nu_3$  ( $F_2C$  scissors). They have obtained the vibrational frequencies of 1660, 790, and 370  $cm^{-1}$ , which have been characterized as the C=C stretching, C-F stretching and C=C-F bending modes, respectively. The calculated values are overestimated about 15.7–19.7% in comparison with their values. Sell and Kuppermann [4] have also reported the frequencies of 1710, 820, and 400  $cm^{-1}$ . Comparing these values, we overestimate about 10.8–14.5%. The vibrational excitations of the  $\nu_1$  mode have a strong intensity. This situation is connected with the change in geometry. It is found from Table 1 that the C=C bond becomes long, the C-F bond becomes short and the C=C-F angle becomes narrow. Tables 1 and 5 show that the magnitude of the change is larger than that of the classical half-amplitude of the

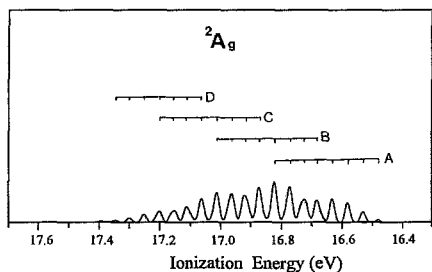


Fig. 6

Fig. 6. The theoretical intensity curves of ionization of the  ${}^2A_g$  state with a half-width of 0.02 eV

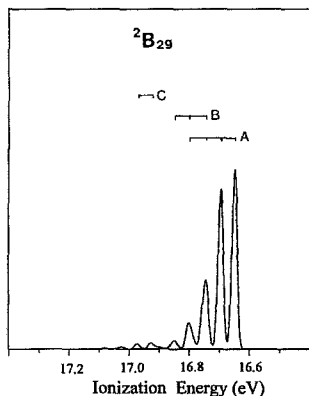


Fig. 7

Fig. 7. The theoretical intensity curves of ionization of the  ${}^2B_{2g}$  state with a half-width of 0.02 eV

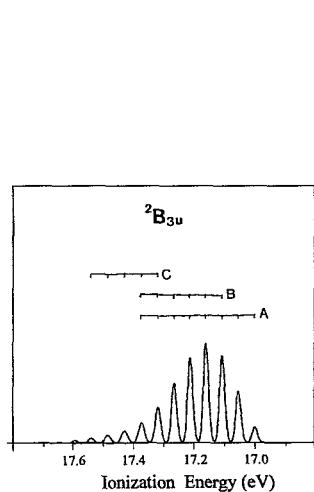


Fig. 8

Fig. 8. The theoretical intensity curves of ionization of the  ${}^2B_{3u}$  state with a half-width of 0.02 eV

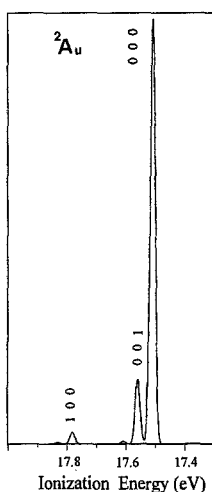


Fig. 9

Fig. 9. The theoretical intensity curves of ionization of the  ${}^2A_u$  state with a half-width of 0.02 eV

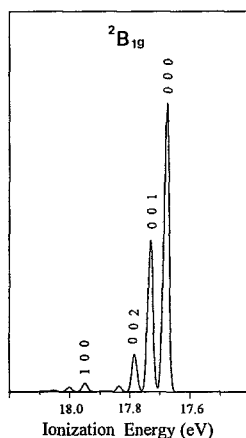


Fig. 10

Fig. 10. The theoretical intensity curves of ionization of the  ${}^2B_{1g}$  state with a half-width of 0.02 eV

zeor-point vibrational level. Table 4 shows that the character of the  $\nu_1$  mode is a mixture of the C=C stretching, C-F stretching, and C=C-F bending motions, and that the phase of the motion is consistent with that of the change in geometry by ionization. Thus, higher vibrational excitations of the  $\nu_1$  mode become important.

The vertical ionization (VI) energy is defined as an ionization energy with a maximum transition probability [16]. In the 15.9–17.0 eV region, Brundle et al. have reported the four VI energies of 15.95, 16.4, 16.6, and 16.9 eV. The present calculation shows that the five ionic states of  ${}^2A_g$ ,  ${}^2B_{2g}$ ,  ${}^2B_{3u}$ ,  ${}^2A_u$ , and  ${}^2B_{1g}$  contribute to the spectrum in this region. Each contribution on the spectrum

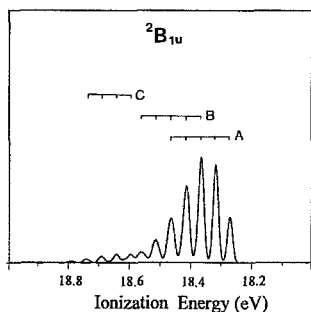


Fig. 11

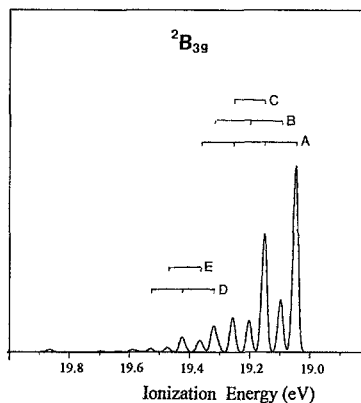


Fig. 12

Fig. 11. The theoretical intensity curves of ionization of the  ${}^2B_{1u}$  state with a half-width of 0.02 eV  
 Fig. 12. The theoretical intensity curves of ionization of the  ${}^2B_{3g}$  state with a half-width of 0.02 eV

Table 5. Vibrational levels of the  ${}^2B_{2u}$  state

| IE    | Progressions |        |        |
|-------|--------------|--------|--------|
|       | A            | B      | C      |
| 9.67  | M(000)       |        |        |
| 9.72  |              | W(001) |        |
| 9.78  |              |        | W(010) |
| 9.91  | S(100)       |        |        |
| 9.97  |              | W(101) |        |
| 10.03 |              |        | W(110) |
| 10.15 | S(200)       |        |        |
| 10.21 |              | W(201) |        |
| 10.27 |              |        | M(210) |
| 10.40 | S(300)       |        |        |
| 10.45 |              | W(301) |        |
| 10.51 |              |        | M(310) |
| 10.64 | S(400)       |        |        |
| 10.70 |              | W(401) |        |
| 10.75 |              |        | M(410) |
| 10.88 | M(500)       |        |        |
| 10.94 |              | W(501) |        |
| 11.00 |              |        | W(510) |
| 11.13 | W(600)       |        |        |
| 11.24 |              |        | W(610) |

Intensity is classified into *S*, *M* or *W* according to the magnitude of FCF as follow: *S*:  $0.14 > \text{FCF} > 0.09$ , *M*:  $0.05 > \text{FCF} > 0.03$ , and *W*:  $0.03 > \text{FCF} > 0.005$

is illustrated in Fig. 4 where the four maxima are found. It shows that the  ${}^2B_{2g}$ ,  ${}^2B_{3u}$ ,  ${}^2A_u$ , and  ${}^2B_{1g}$  states contribute to the four maxima. It is found from Fig. 7 that the first and second peaks of the  ${}^2B_{2g}$  state have almost the same intensity. The VI energy of  ${}^2B_{2g}$  should correspond to the average energy of the first and second

**Table 6.** Vibrational levels of the  ${}^2A_g$  state

| IE          | Progressions   |                |                |                |
|-------------|----------------|----------------|----------------|----------------|
|             | <i>A</i>       | <i>B</i>       | <i>C</i>       | <i>D</i>       |
| 16.79       | <i>W</i> (000) |                |                |                |
| 16.84       | <i>W</i> (001) |                |                |                |
| 16.89       | <i>M</i> (002) |                |                |                |
| 16.94       | <i>M</i> (003) |                |                |                |
| 16.98–16.99 | <i>M</i> (004) | <i>W</i> (100) |                |                |
| 17.03–17.04 | <i>W</i> (005) | <i>M</i> (101) |                |                |
| 17.08–17.10 | <i>W</i> (006) | <i>M</i> (102) |                |                |
| 17.13–17.15 | <i>W</i> (007) | <i>S</i> (103) |                |                |
| 17.17–17.18 |                | <i>M</i> (104) | <i>W</i> (200) |                |
| 17.22–17.23 |                | <i>M</i> (105) | <i>M</i> (201) |                |
| 17.27–17.28 |                | <i>W</i> (106) | <i>M</i> (202) |                |
| 17.32–17.34 |                | <i>W</i> (107) | <i>M</i> (203) |                |
| 17.37       |                |                | <i>M</i> (204) |                |
| 17.41–17.42 |                |                | <i>M</i> (205) | <i>W</i> (301) |
| 17.46–17.47 |                |                | <i>W</i> (206) | <i>W</i> (302) |
| 17.51–17.53 |                |                | <i>W</i> (207) | <i>W</i> (303) |
| 17.56       |                |                |                | <i>W</i> (304) |
| 17.61       |                |                |                | <i>W</i> (305) |
| 17.66       |                |                |                | <i>W</i> (306) |

Intensity is classified into *S*, *M*, or *W* according to the magnitude of FCF as follows: *S*:  $0.09 > \text{FCF} > 0.08$ , *M*:  $0.07 > \text{FCF} > 0.03$ , and *W*:  $0.03 > \text{FCF} > 0.005$

**Table 7.** Vibrational levels of the  ${}^2B_{2g}$  state

| IE          | Progressions   |                |                |
|-------------|----------------|----------------|----------------|
|             | <i>A</i>       | <i>B</i>       | <i>C</i>       |
| 16.92       | <i>S</i> (000) |                |                |
| 16.97       | <i>S</i> (001) |                |                |
| 17.01–17.03 | <i>S</i> (002) | <i>M</i> (010) |                |
| 17.06–17.07 | <i>W</i> (003) | <i>M</i> (011) |                |
| 17.12       |                | <i>W</i> (012) |                |
| 17.20       |                |                | <i>W</i> (100) |
| 17.24       |                |                | <i>W</i> (101) |

Intensity is classified into *S*, *M*, or *W* according to the magnitude of FCF as follows: *S*:  $0.36 > \text{FCF} > 0.10$ , *M*:  $0.06 > \text{FCF} > 0.03$ , and *W*:  $0.03 > \text{FCF} > 0.01$

peaks. Figure 8 shows that the fourth peak of the  ${}^2B_{3u}$  state has the maximum intensity. Figures 9 and 10 indicate that the O–O transitions of the  ${}^2A_u$  and  ${}^2B_{1g}$  states have the maximum transition probability. Therefore, the estimated maxima of the  ${}^2B_{2g}$ ,  ${}^2B_{3u}$ ,  ${}^2A_u$ , and  ${}^2B_{1g}$  states are found at 16.95, 17.42, 17.76, and 17.91 eV, respectively. Comparing the calculated maxima to the observed ones, we overestimate by 1.00, 1.02, 1.16, and 1.01 eV. Theoretical intensity curve of

**Table 8.** Vibrational levels of the  ${}^2B_{3u}$  state

| IE          | Progressions   |                |                |
|-------------|----------------|----------------|----------------|
|             | <i>A</i>       | <i>B</i>       | <i>C</i>       |
| 17.26       | <i>W</i> (000) |                |                |
| 17.31       | <i>S</i> (001) |                |                |
| 17.37       | <i>S</i> (002) |                |                |
| 17.42       | <i>S</i> (003) | <i>W</i> (011) |                |
| 17.47       | <i>S</i> (004) | <i>W</i> (012) |                |
| 17.52       | <i>S</i> (005) | <i>W</i> (013) |                |
| 17.58–17.59 | <i>M</i> (006) | <i>W</i> (014) | <i>W</i> (101) |
| 17.63–17.64 | <i>W</i> (007) | <i>W</i> (015) | <i>W</i> (102) |
| 17.68–17.69 | <i>W</i> (008) |                | <i>W</i> (103) |
| 17.75       |                |                | <i>W</i> (104) |
| 17.80       |                |                | <i>W</i> (105) |

Intensity is classified into *S*, *M*, or *W* according to the magnitude of FCF as follows: *S*:  $0.2 > \text{FCF} > 0.1$ , *M*:  $0.06 > \text{FCF} > 0.03$ , and *W*:  $0.03 > \text{FCF} > 0.007$

**Table 9.** Vibrational levels of the  ${}^2B_{1u}$  state

| IE          | Progressions   |                |                |
|-------------|----------------|----------------|----------------|
|             | <i>A</i>       | <i>B</i>       | <i>C</i>       |
| 18.52       | <i>S</i> (000) |                |                |
| 18.57       | <i>S</i> (001) |                |                |
| 18.61–18.63 | <i>S</i> (002) | <i>W</i> (010) |                |
| 18.66–18.67 | <i>S</i> (003) | <i>M</i> (011) |                |
| 18.71–18.72 | <i>M</i> (004) | <i>M</i> (012) |                |
| 18.75–18.77 | <i>W</i> (005) | <i>M</i> (013) |                |
| 18.80–18.81 |                | <i>W</i> (014) | <i>W</i> (100) |
| 18.85       |                |                | <i>W</i> (101) |
| 18.89       |                |                | <i>W</i> (102) |
| 18.94       |                |                | <i>W</i> (103) |

Intensity is classified into *S*, *M*, or *W* according to the magnitude of FCF as follows: *S*:  $0.21 > \text{FCF} > 0.09$ , *M*:  $0.06 > \text{FCF} > 0.03$ , and *W*:  $0.03 > \text{FCF} > 0.006$

the  ${}^2A_g$  state shows a broad band and overlaps to the bands of the  ${}^2B_{2g}$  and  ${}^2B_{3u}$  states.

The theoretical intensity curve of the  ${}^2A_g$  state is illustrated in Fig. 6 and the four vibrational progressions are found. The assignment of the four progression is given in Table 6 where a series of the long progressions of (000)–(007), (100)–(107), (200)–(207) and (301)–(306) are found. In this state, the vibrational excitations of the  $\nu_1$  and  $\nu_3$  modes are important. This situation is ascribed to the large geometrical change in the C=C, C=C distance, and C=C–F angle. The C=C bond becomes long, the C–F bond becomes short, and the C=C–F angle becomes narrow. The character of the  $\nu_1$  mode is a mixture of the C=C stretching, C–F stretching, and C=C–F bending motions, and that the phase of the motion is

**Table 10.** Vibrational levels of the  ${}^2B_{3g}$  state

| IE          | Progressions   |                |                |                |                |
|-------------|----------------|----------------|----------------|----------------|----------------|
|             | <i>A</i>       | <i>B</i>       | <i>C</i>       | <i>D</i>       | <i>E</i>       |
| 19.25       | <i>S</i> (000) |                |                |                |                |
| 19.30       |                | <i>S</i> (001) |                |                |                |
| 19.35       | <i>S</i> (010) |                | <i>W</i> (002) |                |                |
| 19.40       |                | <i>M</i> (011) |                |                |                |
| 19.45–19.46 | <i>M</i> (020) |                | <i>W</i> (012) |                |                |
| 19.51–19.52 |                | <i>W</i> (021) |                | <i>M</i> (100) |                |
| 19.56–19.57 | <i>W</i> (030) |                |                |                | <i>W</i> (101) |
| 19.63       |                |                |                | <i>W</i> (110) |                |
| 19.67       |                |                |                |                | <i>W</i> (111) |
| 19.73       |                |                |                | <i>W</i> (120) |                |

Intensity is classified into *S*, *M*, or *W* according to the magnitude of FCF as follows: *S*:  $0.38 > \text{FCF} > 0.10$ , *M*:  $0.06 > \text{FCF} > 0.03$ , and *W*:  $0.03 > \text{FCF} > 0.007$

consistent with that of the change in geometry by ionization. The magnitude of the change in the C=C–F angle is large about four times of the classical half-amplitude of the zero-point vibrational level. The character of the  $\nu_3$  mode is the C=C–F bending motion.

The theoretical intensity curve of the  ${}^2B_{2g}$  state is shown in Fig. 7 where the three progressions are recognized. It is found from Table 7 that the short progression of (000)–(003) has strong intensity. The vibrational spacing is due to the frequency of the  $\nu_3$  mode which value is 0.046 eV. Thus, the theoretical intensity curve with a half-width of 0.08 eV is recognized as a sharp band.

Figure 8 shows the theoretical intensity curve of the  ${}^2B_{3u}$  state where the three vibrational progressions are found. Table 8 shows an interpretation of these progressions. The vibrational excitation of the  $\nu_3$  mode is important and the progression of (000)–(008) series has strong intensity. This is connected with the geometrical change in the C=C–F angle. Only the magnitude of the change in the C=C–F angle is larger than that of the classical half-amplitude of the zero-point vibrational level (compare Tables 1 and 5).

The theoretical intensity curve of the  ${}^2A_u$  state is illustrated in Fig. 9 where the O–O transition is very strong intensity. The FCF of the O–O transition is 0.84. This is connected with small change in the geometry. The magnitude of the change is smaller than that of the classical half-amplitude of the zero-point vibrational level (compare Tables 1 and 4).

The spectrum of the  ${}^2B_{1g}$  state also shows a very sharp feature as illustrated in Fig. 10 where a very short progression of (000)–(002) is found. The vibrational excitation of the  $\nu_3$  mode is also connected with the geometrical change in the C=C–F angle. The magnitude of the change is slightly large compared to that of the classical half-amplitude of the zero-point vibrational level (compare Tables 1 and 4).

The PE spectrum at 17.5–18 eV region should be assigned to the  ${}^2B_{1u}$  state. The theoretical intensity curve of the  ${}^2B_{1u}$  state is shown in Fig. 11. Brundle et al. have reported the AI energy of 17.50 eV. The calculated energy of the O–O transition is 18.52 eV, which is overestimated by 1.02 eV compared to the observed one. The observed spectrum shows the vibrational structure. An interpretation of the

vibrational structure has been reported by Brundle et al. They have found the two progressions of (000)–(040) and (001)–(041). They have reported no frequencies of the  $\nu_2$  and  $\nu_3$  modes. Lake and Thompson [1] have given the frequencies of 740 and 330  $\text{cm}^{-1}$  for the  $\nu_2$  and  $\nu_3$  modes, respectively. The calculated frequencies are 853 and 380  $\text{cm}^{-1}$ , which are overestimated by 15%. Three vibrational progressions are found and the assignment is given in Table 9. The vibrational progression of (000)–(005) has strong intensity, that of (010)–(014) has medium intensity, and that of (100)–(103) has weak intensity. The present assignment of the vibrational progressions does not agree with that by Brundle et al. The vibrational excitation of the  $\nu_3$  mode is important in this work, while that of the  $\nu_2$  mode is important in their assignment. The vibrational excitation of the  $\nu_3$  mode is connected with the geometrical change by ionization. Only the magnitude of the change in the C=C–F angle is larger than the classical half-amplitude of the zero-point vibrational level (compare Tables 1 and 4).

In the region of 18–19 eV, PE spectrum has been observed. This band should correspond to the  ${}^2\text{B}_{3g}$  state. The theoretical intensity curve of the  ${}^2\text{B}_{3g}$  state is given in Fig. 12 where the five short progressions are found. Table 10 gives the assignment of each progression. The progression of (000)–(030) has strong intensity and that of (001)–(021) has medium intensity. Brundle et al. have reported the VI energy of 18.21 eV. The present calculation shows that the O–O transition has the maximum intensity and the O–O transition energy is 19.25 eV. Therefore, the observed energy of 18.21 eV should correspond to the O–O ionization energy. Comparing the calculated energy to the observed one, we overestimate by 1.04 eV. In this state, the excitations of the  $\nu_2$  mode mainly contribute to the intensity. This situation is connected with a large geometrical change in the C–F bond length. Only the magnitude of the change in the C–F bond length is larger than that of the classical half-amplitude of the zero-point vibrational level. Therefore the C–F stretching mode contributes mainly to the intensity.

#### 4. Conclusion

The molecular equilibrium structures and vibrational frequencies have been calculated for the ground and lower eight ionic states. We have obtained the theoretical intensity curve by using the FCFs. The total theoretical intensity curves are in good agreement with the observed PE spectrum.

The lowest ionic state is the  ${}^2\text{B}_{2u}$  state of which PE spectrum has a well resolved vibrational structure. The vibrational progression of the (000)–(600) has strong intensity. This situation is connected with a large change in geometry and the character of the  $\nu_1$  mode. It is found that the C=C bond becomes long, the C–F bond becomes short, and the C=C–F angle becomes narrow. The character of the  $\nu_1$  mode is a mixture of the C=C stretching, C–F stretching, and the C=C–F bending motions, and that the phase of the motion is consistent with that of the change in geometry by ionization.

In the 15.9–17.0 eV region, the four maximum peaks at 15.95, 16.4, 16.6, and 16.9 eV have been observed in the PE spectrum. The present calculation shows that the five ionic states of  ${}^2\text{A}_g$ ,  ${}^2\text{B}_{2g}$ ,  ${}^2\text{B}_{3u}$ ,  ${}^2\text{A}_u$ , and  ${}^2\text{B}_{1g}$  contribute to this region. Theoretical intensity curve of the  ${}^2\text{A}_g$  state shows a broad band but those of the  ${}^2\text{B}_{2g}$ ,  ${}^2\text{A}_u$ , and  ${}^2\text{B}_{1g}$  states show very sharp bands. We propose that the peak at 15.95 eV should correspond to the average energy of the (000) and (001) levels of the  ${}^2\text{B}_{2g}$  state. The peak at 16.4 eV should be the (003) level of the  ${}^2\text{B}_{3u}$  state. The

peaks at 16.6 and 16.9 eV should be the O–O transitions of the  ${}^2A_u$  and  ${}^2B_{1g}$  states, respectively. The band the  ${}^2A_g$  state should overlap to the those of the  ${}^2B_{2g}$  and  ${}^2B_{3u}$  states. The changes in the equilibrium geometrical parameters of the  ${}^2A_u$  and  ${}^2B_{1g}$  states are negligibly so small compared to the magnitudes of the classical half-amplitude that the intensity of the O–O transitions is very strong. For the  ${}^2B_{2g}$  and  ${}^2B_{3u}$  states, the geometrical change in the C=C–F angle is so large that the vibrational progression including the excitation of the  $\nu_3$  mode has strong intensity. A large geometrical change is found in the C=C, C=C distance and C=C–F angle of the  ${}^2A_g$  state. The higher vibrational excitations of the  $\nu_1$  and  $\nu_3$  modes contribute to the spectrum.

The PE spectrum at 17.5–18 eV region should be assigned to the  ${}^2B_{1u}$  state. The vibrational progression of (0 0 0)–(0 0 5) has strong intensity. The vibrational excitation of the  $\nu_3$  mode is connected with a large geometrical change in the C=C–F angle.

The PE spectrum of 18–19 eV region should be assigned to the  ${}^2B_{3g}$  state. The present calculation propose that the O–O transition has the maximum intensity and the observed energy of 18.21 eV should be the O–O ionization energy.

*Acknowledgements.* Computation has been carried out on HITAC M-680H systems at the Center for Information Processing Education of Hokkaido University and IBM RISC system/6000 at the Faculty of Bioindustry of Tokyo University of Agriculture. The authors are grateful to Dr. M. Yoshimine, Dr. E. Miyosi, Dr. T. Noro and Dr. T. Sakai for helpful suggestions.

## References

1. Lake RF, Thompson H (1970) Proc Roy Soc Ser A 315:323
2. Brundle CR, Robin MB, Kuebler NA, Basch H (1972) J Am Chem Soc 94:1451
3. Sell JA, Mintz DM, Kuppermann A (1978) Chem Phys Lett 58:601
4. Sell JA, Kuppermann A (1979) J Chem Phys 71:4703
5. Bieri G, Åsbrink L, Niessen WV (1981) J Electr Spectr Rel Phen 23:281
6. Heaton MM, El-Talbi MR (1986) J Chem Phys 85:7198
7. Tatewaki H, Huzinaga S (1980) J Comput Chem 1:205
8. Takeshita K (1987) J Chem Phys 86:329
9. Takeshita K, Sasaki F (1981) Library program at the Hokkaido University Computing Center (in Japanese). GRAMOL includes the Program JAMOL3 of the RHF calculation written by Kashiwagi H, Takada T, Miyoshi E, Obara S for the Library program at the Hokkaido University Computing Center 1977 (in Japanese)
10. Lengsfeld BH III (1980) J Chem Phys 73:382
11. Liu B, Yosimine M (1981) J Chem Phys 74:612
12. Lengsfeld BH III, Liu B (1981) J Chem Phys 75:478
13. Carlos JL JR, Karl RR JR, Bauer SH (1974) J Chem Soc Faraday Trans 2 70:177
14. Nielsen JR, Claassen HH, Smith DC (1950) J Chem Phys 18:812
15. Morino Y, Kuchitsu K (1952) J Chem Phys 21:1809
16. Turner DW, Baker AD, Baker C, Brundle CR (1970) Molecular photoelectron spectroscopy. Wiley, London